Research Article

Organosilane and Lignosulfonate Stabilization of Roads Unbound: Performance during a Two-Year Time Span

Diego Maria Barbieri [iD],[1] **Baowen Lou** [iD],[1,2] **Hao Chen** [iD],[1] **Benan Shu** [iD],[3] **Fusong Wang** [iD],[4] **and Inge Hoff** [iD][1]

[1]*Norwegian University of Science and Technology, Department of Civil and Environmental Engineering, Høgskoleringen 7A, Trondheim, 7491, Trøndelag, Norway*
[2]*Chang'an University, School of Materials and Science Engineering, Nan Er Huan Road (Mid-Section), Xi'an 710064, Shaanxi, China*
[3]*Foshan Transportation Science and Technology Co. Ltd, Kuiqi Second Road 18, Foshan 528000, Guangdong, China*
[4]*State Key Laboratory of Silicate Materials for Architectures, Wuhan University of Technology, Luoshi Road 122, Wuhan 430070, Hubei, China*

Correspondence should be addressed to Diego Maria Barbieri; diego.barbieri@ntnu.no

The construction of the new Norwegian E39 highway comprises the excavation of extended tunnelling systems, which lead to a tremendous amount of blasted rocks. Among others, a sustainable cost-benefit application of these resources is represented by their local use as construction material in the unbound layers of the roads. Two types of nontraditional additives are investigated to improve the mechanical properties of aggregates; this is particularly useful for those rocks that do not fulfil the design requirements in their natural status. This work focuses on the field application of two innovative stabilizing technologies based on organosilane and lignosulfonate. The performance of these additive agents is characterized by considering three typical road base layer sections built on purpose according to real practice and added with water (no treatment), organosilane, and lignosulfonate. The test sections are subjected to climatic actions only as neither traffic nor surface courses are applied. With the investigation covering two years, the layers' stiffness, deformation, and resistance to penetration are evaluated by employing a light-weight deflectometer and dynamic cone penetrometer. Both organosilane and lignosulfonate significantly enhance the mechanical properties of the treated base layers.

1. Introduction

By fulfilling the "ferry-free coastal highway route E39" project, the Norwegian Public Roads Administration (NPRA) aims at improving the viability along the southwestern Norwegian coast from Trondheim to Kristiansand coast for an overall length of about 1100 km [1, 2]. The project comprises the creation of extended tunnelling systems, thus leading to the generation of a tremendous amount of blasted rocks. Among others, a sustainable way to employ these natural resources as construction materials is represented by their use in the unbound layers of the roads built in the proximity of the tunnel infrastructures. This solution

would engender remarkable advantages from several points of view and curtail the consumption of natural resources and related pollutant emissions [3–7]. In addition, the importance of sustainable and environmentally friendly solutions is becoming more and more significant in the world as well as in Norway as the country pursues climate neutrality [8].

To avoid encountering premature damage [9], the Norwegian pavement design manual specifies some requirements for unbound granular materials (UGMs) to be used in the road unbound layers [10, 11]; among others, the Los Angeles (LA) value [12] and microdeval (MDE) value [13] are usually the most stringent criteria to be fulfilled [14]. The geology spread along the highway alignment is largely

various and comprises both rocks that meet the design requirements ("strong" aggregates, generally igneous rocks), while other rocks ("weak" aggregates, generally sedimentary and metamorphic rocks) do not [15].

Several traditional stabilization technologies have been thoroughly characterized to improve the mechanical properties of unbound layers, for example, cement, bitumen, fly ash, lime, and gypsum [16–21]. Recently, two nontraditional stabilizing agents have shown promising results to improve the mechanical response of crushed rock aggregates [22–24]. The two additives are based on organosilane and lignosulfonate, here also referred to as polymer-based (P) agent and lignin-based (L) agent, respectively.

Considering that the previous investigations dealing with the stabilization potentials of the P-based and L-based products were largely based on laboratory tests performed on clayey and silty materials [25–32], this study expands the previous findings by encompassing a field test on crushed rock aggregates covering the time span of two years. Three typical base road sections were built according to the actual Norwegian construction practice and added with water (no treatment), organosilane and lignosulfonate, respectively. The test sections were only subjected to climatic actions as neither traffic nor surface courses were applied. Across a time span of two years, the stiffness and the deformation properties have been assessed using a light-weight deflectometer (LWD) [33] and dynamic cone penetrometer (DCP) [34]. Aggregates that fulfil standard code requirements were used in this study as performing the field test with enough quantities of "weak" aggregates was not feasible.

2. Materials and Methods

2.1. Crushed Rock Aggregates. The field test was performed in the Vassfjellet locality close to Trondheim (Trøndelag, Norway). The rocks available in this place, mainly characterized by metamorphic reactions, are particularly rich in gabbro/metagabbro and greenschist [35]; moreover, they are commonly employed for road construction in the central part of Norway [36]. X-ray diffractometry (XRD) and X-ray fluorescence (XRF) analyses were preliminarily performed to thoroughly characterize the aggregates. A Bruker D8 Advance instrument displaying a cobalt tube with wavelength of 1.79 Å was used to perform XRD analysis and examine the composition based on the Rietveld approach, and the proportions of the most abundant minerals are reported in Figure 1. Hornblende (amphibole), chlorite, albite (feldspar), and clinozoisite (epidote) were the predominant minerals. The XRF analysis was attained employing a PANalytical Zetium 4 kW X-ray spectrometer. The major elements as well as the Loss On Ignition (LOI) are reported in Table 1, and silicon was the major component.

According to the requirements specified by the Norwegian pavement design manual N200 [10, 11], crushed rocks can be used as construction material in the base and in the subbase of a road considering the results of the Los Angeles standard test (LA value) and the microdeval standard test (MDE value). As the threshold values for base layers are set to 30 and 15, the crushed rocks deriving from Vassfjellet fulfil the code requirements (LA = 18.2 and MDE = 14.2). Anyway, this did not obstruct the general goal of the study, namely, to evaluate whether organosilane and lignosulfonate can enhance the mechanical properties of crushed rocks; consequently, the achieved improvements may even be greater for poorer rock aggregates. Figure 2(a) displays the grain curve used in the field investigation as well as the gradation range [37]; the maximum aggregate size was 32 mm. The optimum moisture content (OMC) was also evaluated [38] and found equal to 5% for bulk density approximately equal to 2.5 t/m^3 as depicted in Figure 2(b).

2.2. Stabilization Technologies. The existing nontraditional technologies effective for stabilization of coarse-graded roads unbound can be categorized as [39]: synthetic polymer, organic nonpetroleum, organic petroleum, clay, and brine salt. Organosilane is a synthetic polymer, whereas lignosulfonate is an organic nonpetroleum product. The safety data sheets of both the additives do not report any environmental hazards, and the degradation is environmentally acceptable [40, 41]. Currently, the largest amount of research focuses on polymeric and plant-based technologies as they are the newest stabilization solutions [42].

Polymeric stabilizers were first introduced during the 60s as synthetic monomers with dimension ranging from 0.05 μm to 5 μm in diameter [43, 44]. Their stabilizing process is based on the coalescence, which indicates the creation of a film forming physical bonds after the emulsion evaporation [45]. Polymeric products can be classified as acrylate, polyurethane, styrene butadiene, or acetate [46]. The organosilane is a nanoscale nonleachable and UV- and heat-stable acrylate based on two components, namely an emulsion based on acetic acid and methanol (component C1) and a fine dispersion based on propylene glycol and alkoxy-alkyl silyl (component C2). After combination with the silicates naturally present on the aggregate surface forming siloxane linkages (=Si-O-Si=), the additive promotes the formation of a 4–6-nm layer of hydrophobic alkyl siloxane as depicted in Figure 3 [30, 47–49]. The main physical properties of the organosilane used in this study are reported in Table 2. The chemical bindings are damaged if exposed to base substances [50] or temperature above 200°C [51].

Lignosulfonate is an organic polymer that consists of both hydrophilic and hydrophobic groups; it is a renewable substance deriving from lignin extracted by paper and pulp industries. The product is water soluble and not toxic [25, 28, 52]. Thanks to its cementitious properties, lignosulfonate binds the aggregate particles together as depicted in Figure 4 [31]. When applied as a stabilizer for roads unbound, the potential leaching under wet conditions can be partially hindered by providing a proper surface drainage or surface treatment. The main physical properties of the lignosulfonate used in this study are reported in Table 3. Considering the engendered physical cementation action (minor or no chemical effects), it has been indicated that the stabilization process may augment with the decreased surface area,
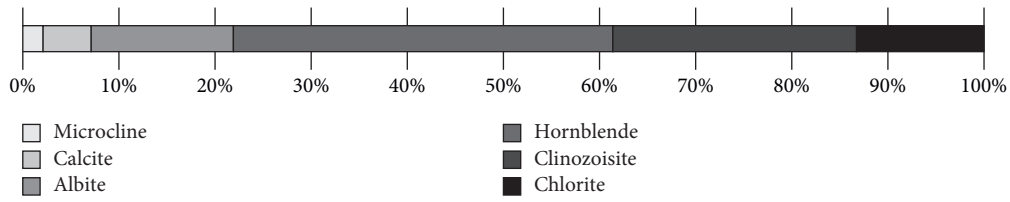
FIGURE 1: Bulk mineralogy of crushed rock aggregates.

TABLE 1: Chemical composition of crushed rock aggregates (weight percent of major oxides).

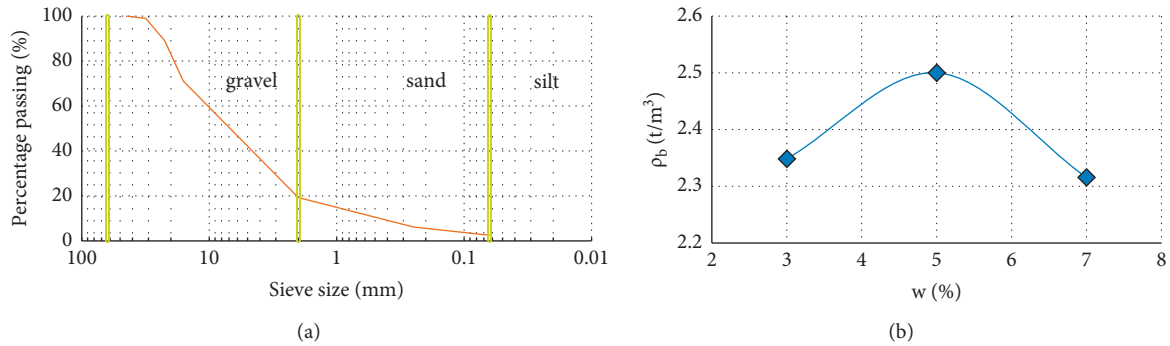| SiO_2	Al_2O_3	Fe_2O_3	CaO	MgO	Na_2O	TiO_2	SO_3	K_2O	LOI
44.1	13.0	12.8	11.5	10.2	1.91	0.91	0.20	0.10	5.01

(a)

(b)

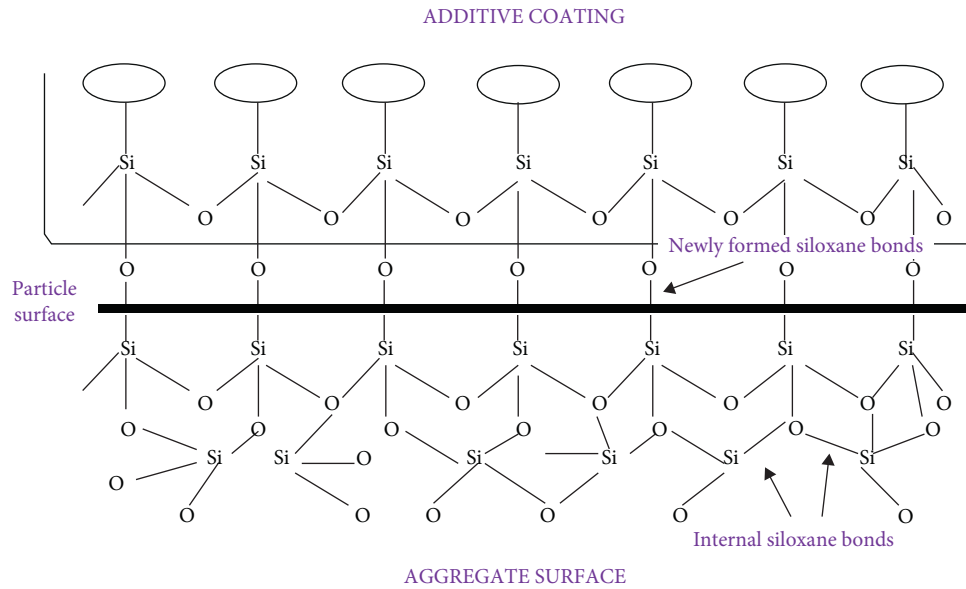FIGURE 2: Grain size distribution curve (a) and assessment of OMC (b).

FIGURE 3: Stabilization mechanism for silicate-containing aggregates with organosilane [30].

TABLE 2: Main physical properties and water contained in organosilane (from technical representatives).

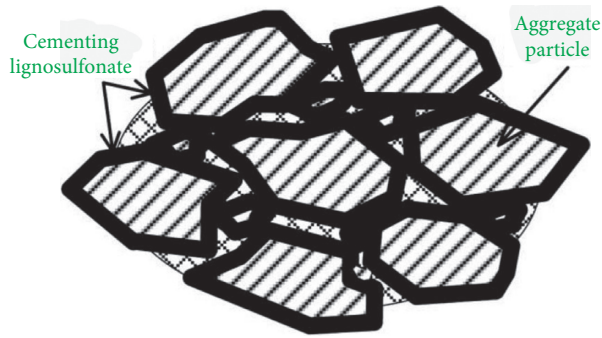|	Component	Freezing point (°C)	Boiling point (°C)	Viscosity (cP @ 30°C)	Density (kg/m³)
P-BASED	**C1**	0	100	20–200	1010
	C2	<−5	188	200–600	1020

FIGURE 4: Stabilization mechanism for aggregates with lignosulfonate [31].

TABLE 3: Main physical properties and water contained in lignosulfonate (from technical representatives).

	Freezing point	Boiling point	Viscosity	Density
	(°C)	(°C)	(cP @ 30°C)	(kg/m^3)
L-BASED	−5–0	100	550	1250

namely, improving when moving from applications for fine-graded soils to coarse-graded aggregates [39].

2.3. Test Sections and Test Procedures. The field test was performed in an open space located in a quarry in Vassfjellet (Trøndelag, Norway). Considering the grain size distribution curve reported in Figure 2(a), three base layer sections were built and were treated according to three different procedures: water only/untreated (section L0), polymer-based additive (location L1), and lignin-based additive (location L2). Width, length, and approximate thickness of each section were 3.5 m × 10 m × 17 cm thick, respectively. The main operational stages to build the road test locations illustrated in Figure 5 were accomplished in May 2018; further information regarding the construction procedure can be found in [24]. Table 4 reports on the amount of the admixtures employed.

The light weight deflectometer (LWD) is a single-person-use portable instrument employed for the determination of the mechanical properties of the test sections and to characterize their spatial distribution [33, 53, 54]. The device used in this investigation is manufactured by the HMP company [55]. The test consists in subjecting the road base layer to a pulse load applied via a steel plate; a geophone records the speed of the plate movement. The LWD is made of the following parts as illustrated in Figure 6: loading mechanism handle (1), release mechanism (2), bubble level (3), guide rod allowing the falling weight to drop from a distance of 72 cm (4), 10-kg drop-weight (5), transportation lock pin (6), and elastic element with prestressed disc springs (7). The load plate is 30 cm in diameter and comprises a cap with a sensor (8), a sensor socket to connect the measuring cable (9), and a load plate carrying handles (10). The sensor which serves to measure the settlement is positioned under the cap (8) of the load plate [56]. The loading mechanism generates a defined impulsive load, and the total settlement

of the layer under the load plate is measured; the maximum impact force is 7.07 kN, the duration of the impact is 17.0 ± 1.5 ms, and the deflection range measured is 0.1 to 2.0 mm ± 0.02 mm. After the completion of three measurements, the deflection transducer (geophone) evaluates the average settlement S_m and the resilient modulus E_{LWD} according to the circular plate half-space theory assuming homogeneous, isotropic, linear elastic material behavior [58,59]. Different from a falling weight deflectometer (FWD) device, the LWD employs a shorter load pulse and a smaller force action [60,61].

The dynamic cone penetrometer (DCP) device was also employed to appraise the stabilizing potentials of P-based and L-based technologies in addition to the LWD in terms of their resistance to penetration. This test was accomplished by driving a metal cone into the base layer by releasing an 8-kg weight from a distance of 575 mm as illustrated in Figure 6 [34, 57]. The DCP was adopted here as a further practical approach to better evaluate the admixtures' performances in addition to the LWD as the DCP results may be correlated to other properties, for example, resilient modulus and bearing capacity [62–64].

LWD measurements were performed daily during the first 50 days starting after construction completion (May and June 2018). Moreover, LWD tests were also carried out from day 110 to day 115 (September 2018), from day 365 to day 370 (May 2019), and from day 730 to day 735 (May 2020) after construction completion. DCP tests were performed during day 115, day 370, and day 735. The field investigation thus covered an overall time span of two years. The LWD and DCP measurements in each location were performed for 15 spots, and average values are presented here.

The measuring operations were accomplished after it had stopped raining in case of precipitation. Skjetlein and Saupstad weather stations daily recorded the precipitation amount and the average, minimum, and maximum temperature [65]; average values are reported in this study according to the distance weighting method [66]. The two chosen weather stations are the closest ones to the test site, being approximately located 5 km away from the quarry.

3. Results and Discussion

3.1. Aggregate Coating and Field Conditions. The surfaces of untreated and treated crushed rocks were probed in the laboratory by two means as depicted in Figure 7. A microscope operating at 40x magnification enabled the reconnaissance of the main minerals, namely amphibole, feldspar, and epidote as reported in Section 2.1. Both the P-based and L-based additive completely covered the aggregates surface. The organosilane was characterized by spherical structures (gas bubbles) created in conjunction with the foaming process, whereas the polygonal structures related to lignosulfonate formed an irregular mesh-shaped coating. Scanning electron microscopy (SEM) analysis was also performed to investigate the microstructure and morphology using an emission current of 10 μA and an acceleration voltage of 10 kV. Both organosilane and lignosulfonate utterly covered the aggregate matrix surface as the smaller fragmented particles were no longer visible.
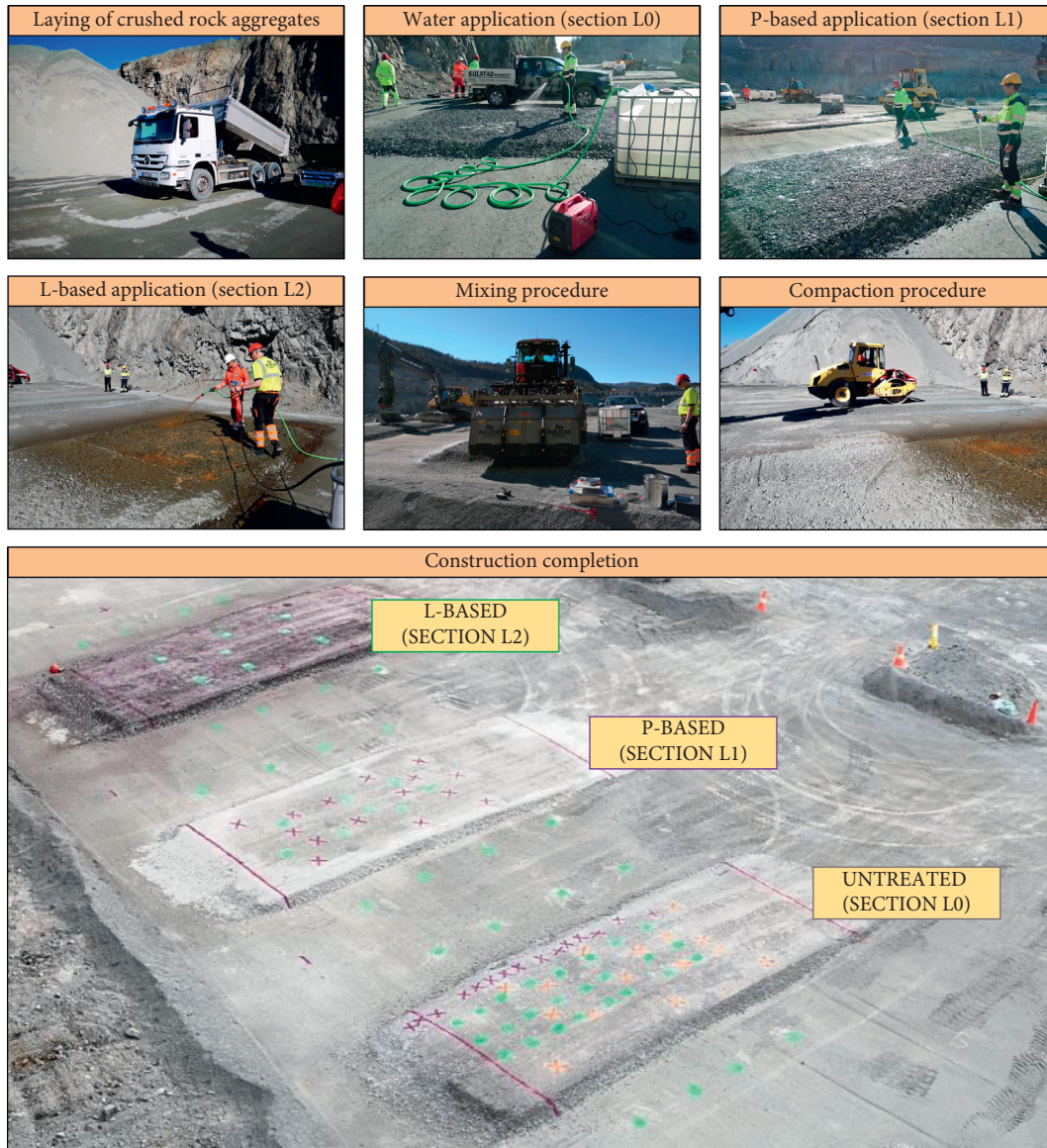
FIGURE 5: Main stages of the construction operations to build the road rest sections.

TABLE 4: Quantity of admixtures used in each location.

Location	Water (kg)	P-based additive (kg)	L-based additive (kg)
L0	500	0	0
L1	500	26 (C1) + 26 (C1)	0
L2	500	0	150

The density of the test sections was evaluated, thanks to the excavation method [67], and the calculated bulk density ρ_b, dry density ρ_d and water content w are displayed in Figure 8. The amount of lignosulfonate used in location L2 was remarkably higher than the admixtures employed in the other two locations; consequently, location L2 was oversaturated, and the measurements here were performed after 5 days.

During the two-year time span, the test sections were exposed to the temperature variations depicted in Figure 9. In this regard, Figure 10 reports more details regarding the time when the LWD and DCP measurements were performed. From day 1 to day 50 (May and June 2018), the average temperature was comprised between 5°C and 20°C with small precipitations (Figure 10(a)); this situation was exceptionally dry and warm for the Norwegian context [68]. Considering the three temporal frames day 110–day 115 (September 2018), day 365–day 370 (May 2019), and day 730–day 735 (May 2020), the average temperatures were 12.5°C, 5.4°C and 10.0°C and the cumulated amounts of precipitation were 13.4 mm, 21.1 mm, and 6.7 mm, respectively (Figures 10(b)–10(d)).
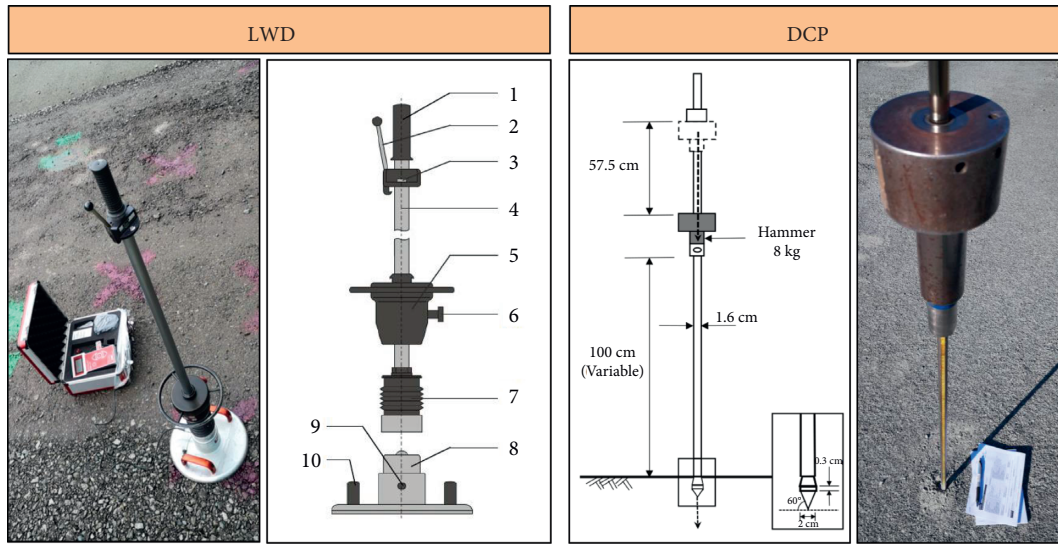
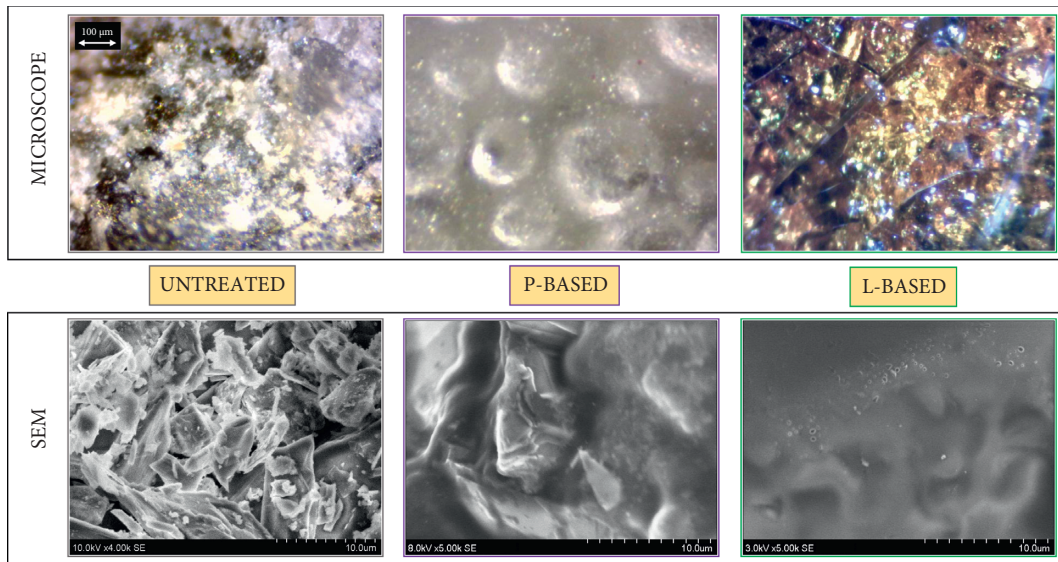FIGURE 6: Components of the LWD and DCP used in the field test [56, 57].

FIGURE 7: Appearance of the surface of crushed rock aggregates probed with the microscope (scale bar 100 μm) and SEM (scale bar 10 μm).

The surface appearance of the three road sections during the two-year time span is depicted in Figure 11. In this regard, the clearest differences regarding the aggregate surfaces could be observed after construction completion when the untreated unbound matrix only contained water and the materials treated with organosilane and lignosulfonate displayed a less rough surface with colors fading to grey and brown, respectively. Afterwards, owing to the complete exposure of the test sections to natural actions, the appearance of the stabilized surfaces became slightly different. Even if after two years, the additives did not completely coat the surface of the crushed rocks, and the presence of a bound matrix could still be clearly observed among the aggregates when inspecting the surface carefully.

3.2. Light Weight Deflectometer Measurements. The first sequence of LWD measurements was performed during the first 50 days after construction completion of the road sections. Figures 12(a) and 12(b) report the resilient modulus E_{LWD} and the settlement S_{LWD}, respectively. During this period, the location L1 treated with organosilane registered the highest E_{LWD} value (163.5 MPa) and the lowest S_{LWD} value (0.14 mm). Meanwhile, the effect of the lignosulfonate became evident at a slower pace (most likely due to the initial oversaturation of location L2) and the highest values of E_{LWD} and S_{LWD} for the lignosulfonate-based treated materials were equal to 133.4 MPa and 0.18 mm, respectively. Moreover, despite the fact that the surfaces of all the test sections were not graded according to a cross profile to promote water discharge, it is worth noting that precipitations exerted a
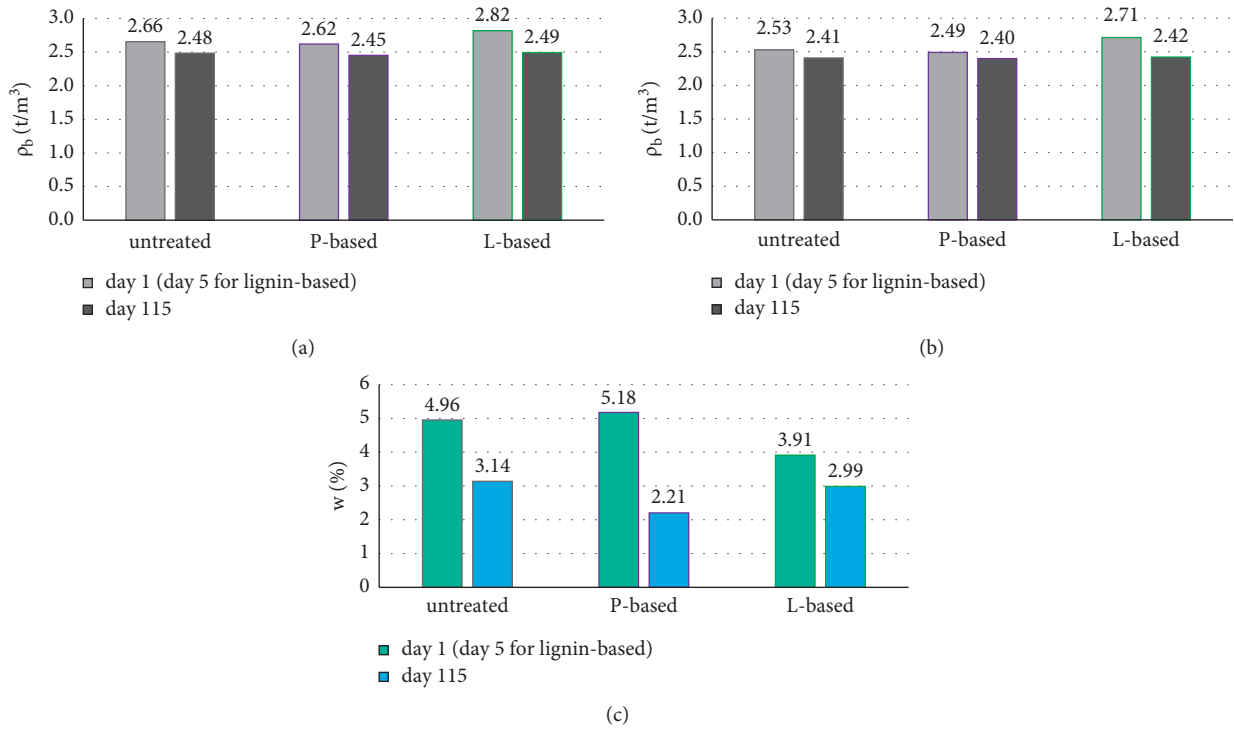
(a)

(b)

(c)

Figure 8: Bulk density (a), dry density (b), and water content (c). of the three test locations after construction and after 115 days [24].

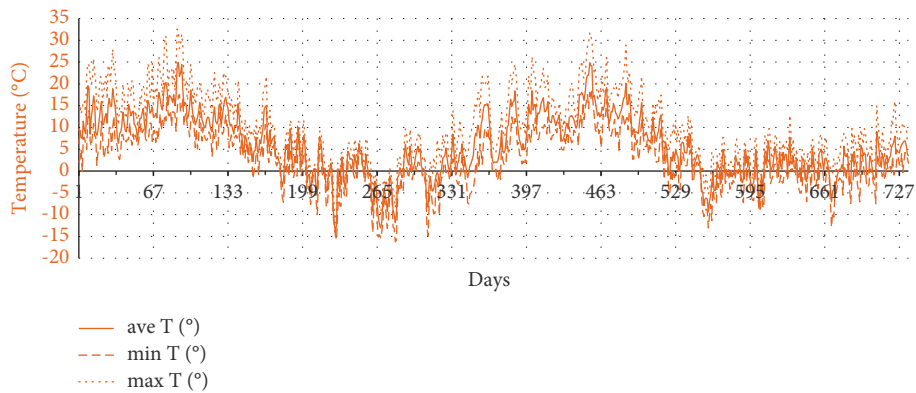Figure 9: Climatic conditions for the two-year time span: average, minimum, and maximum temperature.
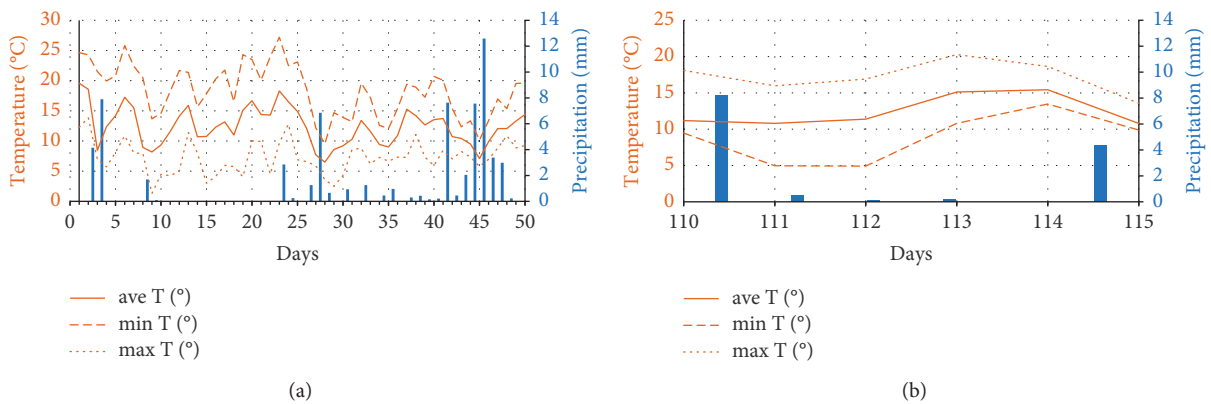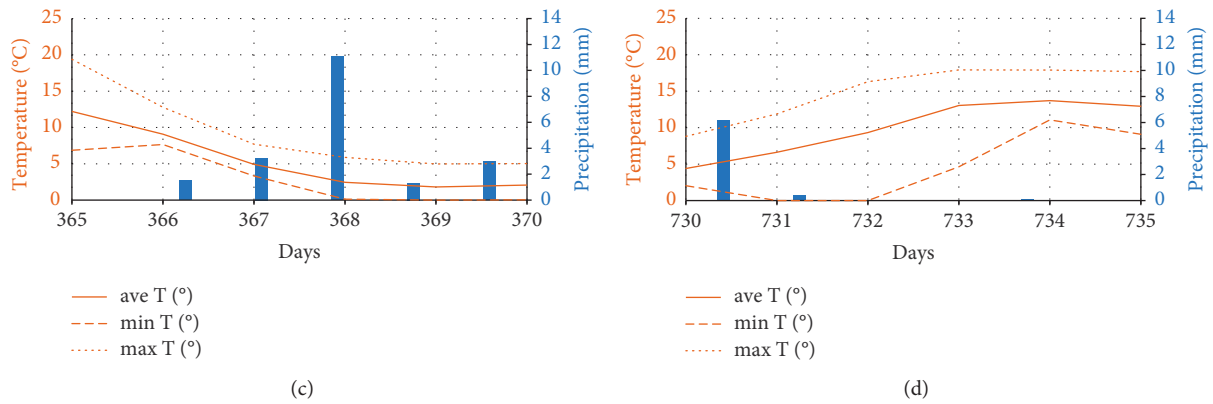

(a)

(b)

Figure 10: Continued.

FIGURE 10: Weather conditions in the field. Day 1–day 50 (a), day 110–day 115 (b), day 365–day 370 (c) [24], and day 730–day 735 (d): average, minimum, and maximum temperature and precipitation.
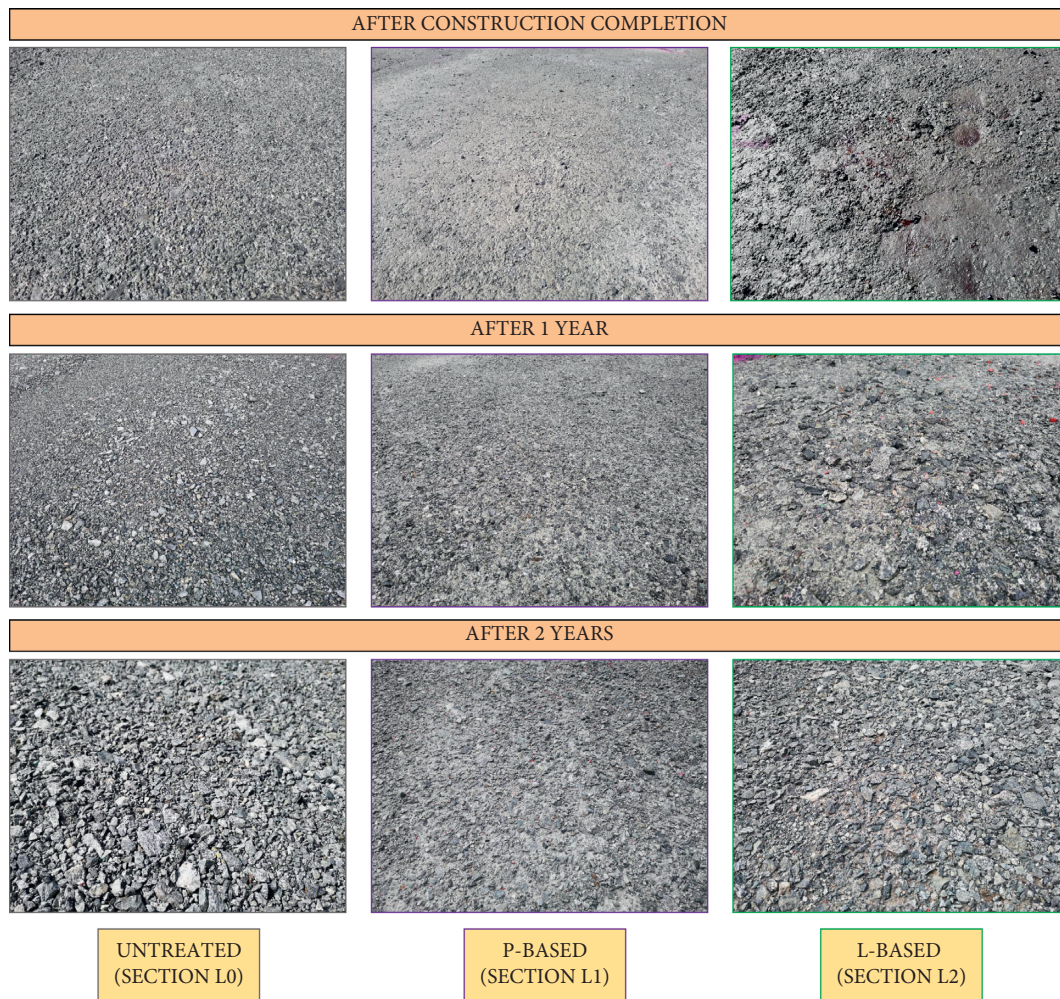

FIGURE 11: Surface appearance of the tested road sections during a two-year time span (the maximum size of the rock aggregates is 32 mm).

major effect only for the untreated location L0, while small daily variations were observed for locations L1 and L2. Figures 12(c)–12(d) report E_{LWD} and S_{LWD}, respectively, during day 110–day 115. These measurements prove that the treated areas had mechanical performances that were significantly higher than location L0. The average values of

E_{LWD} were 42.2 MPa, 102.5 MPa, and 103.9 MPa, and the average values of S_{LWD} were 0.46 mm, 0.22 mm, and 0.23 mm for L0, L1, and L2, respectively. Compared to the measurements related to day 1–day 50, the significant amount of precipitation that took place between day 50 and day 110 could account for the smaller values measured
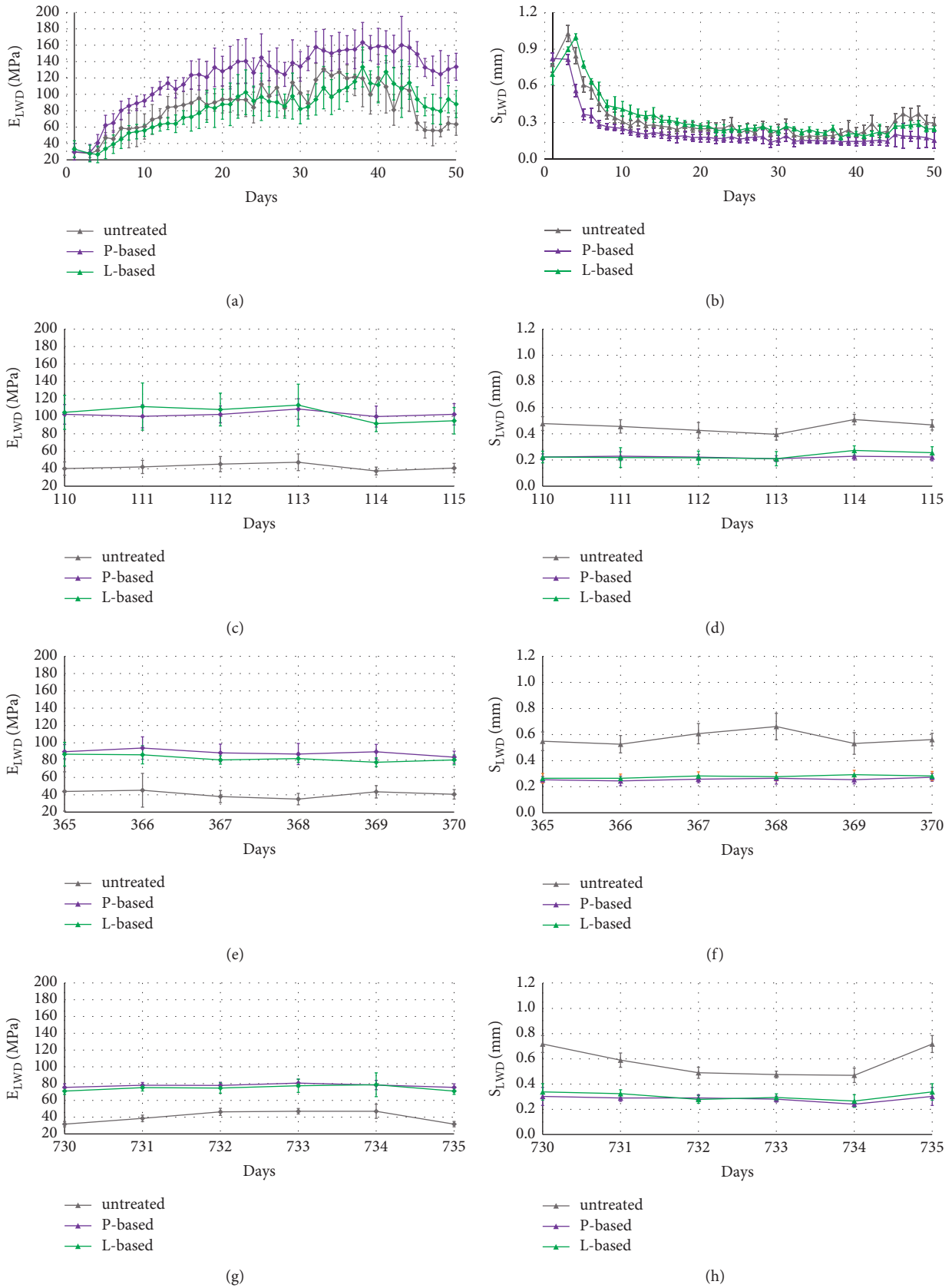
FIGURE 12: Resilient modulus E_{LWD} (a, c, e, g) and settlement S_{LWD} (b, d, f, h) for day 1–day 50, day 110–day 115, day 365–day 370 [24] and day 730–day 735.
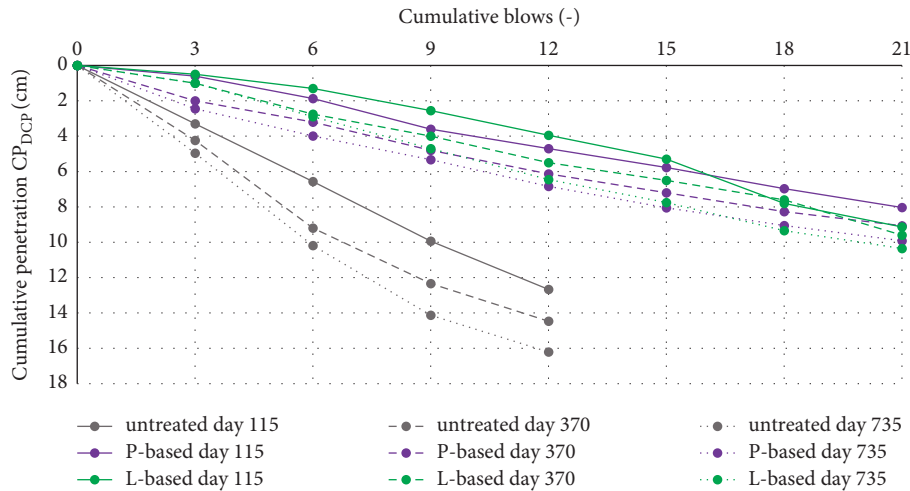
Figure 13: Cumulative penetration CP_{DCP} measured on day 115, day 370 [24], and day 735.
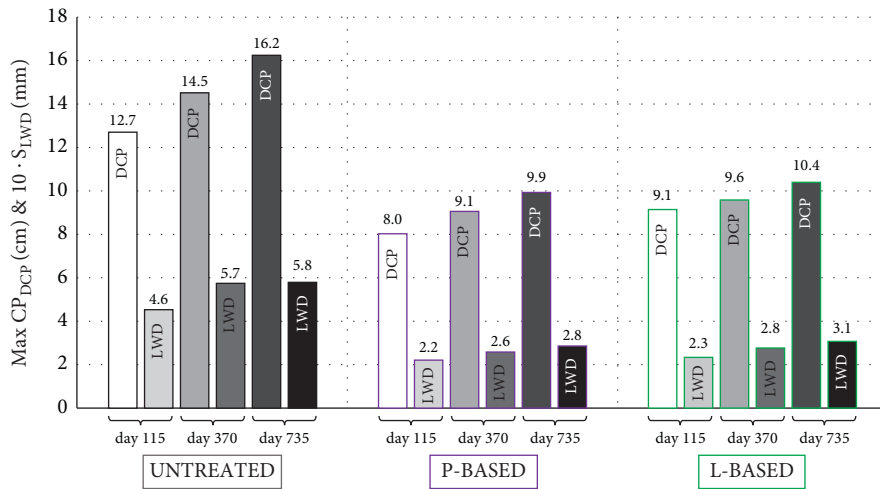

Figure 14: Values of maximum cumulative penetration CP_{DCP} and settlement S_{LWD}.

during day 110–day 115. Figures 12(e)–12(f) display the mechanical performance after one year of construction, namely during day 365–day 370, despite the general decrease in the values of E_{LWD} and S_{LWD}, the treated locations continued to perform much better than the untreated locations. The average values of E_{LWD} were 41.0 MPa, 88.7 MPa, and 82.2 MPa, and the average values of S_{LWD} were 0.57 mm, 0.26 mm, and 0.28 mm for L0, L1, and L2, respectively. Considering the measurements achieved after two years, namely during day 730–day 735, it is evident that both organosilane and lignosulfonate continued to entail positive effects. The average values of E_{LWD} were 40.4 MPa, 77.6 MPa, and 74.7 MPa, and the average values of S_{LWD} were 0.58 mm, 0.28 mm, and 0.31 mm for L0, L1, and L2, respectively.

Considering the whole general trend of the mechanical properties measured during the two-year life span, both organosilane and lignosulfonate performed satisfactorily, attaining better results compared to the untreated material. Referring for example to the resilient modulus, the average values after 115 days, 1 year, and 2 years were 42.2 MPa,

41.0 MPa, and 40.4 MPa for untreated aggregates, 102.5 MPa, 88.7 MPa, and 77.6 MPa for P-based treated materials, and 103.9 MPa, 82.2 MPa, and 74.7 MPa for L-based treated materials, respectively. Even if the stabilized aggregates always performed better than the untreated material, a slowly decreasing mechanical response of the former ones was registered and this phenomenon can be attributed to their complete exposure to atmospheric actions such as rain and snow. For instance, feasible solutions to prevent or reduce this effect would be represented by covering the treated course with an overlying (i.e., bituminous) course or ensuring the presence of a proper water drainage system (e.g., transversal profile and ditches).

3.3. Dynamic Cone Penetrometer Measurements. A DCP test comprised 7 measurement sequences with 3 blows each. Figure 13 displays the depth of cumulative penetration CP_{DCP} measured from the layer surface at the end of each sequence. The results referring to location L0 only comprised 4 sequences, namely 12 blows, as a higher number of blows was enough to penetrate the entire layers' thickness (17 cm). Overall, the

treated locations L1 and L2 were always stiffer than the untreated location L0. Considering the trends across the two-year time span, the location L0 underwent the largest variations; on the other hand, the application of organosilane and lignosulfonate proved to be an effective way to stabilize both locations L1 and L2. Despite the reduction in the mechanical response over time most likely due to the total exposure to climatic actions, the stabilized materials always performed better than the untreated aggregates. As mentioned in Section 3.2, the detrimental effects on the additive effectiveness apported by natural precipitations could be reduced or hindered by implementing some good construction practices.

The results of DCP cumulative penetration and the findings obtained from LWD equipment were in good agreement as both the tests indicated that (i) the stabilized road sections performed better than the untreated area and that (ii) the mechanical response related to organosilane and lignosulfonate gradually reduced over time.

To further characterize the results deriving from the two-testing device, Figure 14 compares the values of maximum cumulative penetration CP_{DCP} and settlement S_{LWD} obtained from DCP and LWD, respectively. Overall, the trends are in good agreement as all the values assessed for each test section tend to increase over time. A relationship between the two quantities can be defined as

$$S_{\text{LWD}}(mm) = a \cdot CP_{\text{DCP}}(mm). \tag{1}$$

Considering the experimental values reported in Figure 14, the calculation employing a least-square method indicates that a value is 0.0032 in this investigation.

4. Conclusions

The study characterized the use of two nontraditional stabilizing agents based on organosilane and lignosulfonate to enhance the mechanical properties of crushed rock aggregates to be employed as construction materials in the unbound layers of road pavements. Organosilane reacted with the silicates naturally present on the aggregate surface forming chemical covalent polar bonds, whereas lignosulfonate physically cemented the aggregate particles together. The surfaces of the treated materials were initially completely covered by the additives as probed with the microscope and SEM. The effectiveness of the stabilizing technologies was evaluated in a field test displaying three base road sections, each of which was added with only water (untreated), organosilane, and lignosulfonate. The test had a temporal duration covering two years, and neither traffic nor surface courses were applied; the layers were only subjected to natural climatic actions. The mechanical properties in terms of stiffness, deformation, and resistance to penetration were characterized by the LWD and DCP. The following conclusions can be drawn:

(1) Both organosilane and lignosulfonate were effective technologies to enhance the mechanical performance of crushed rocks to be used as aggregates in the road base layers. The LWD and DCP measurements performed within the two-year time frame highlighted the persistent effectiveness of the stabilizing agents.

(2) Based on the data collected during the first 50 days, the organosilane had a more rapid stabilizing effect compared to the lignosulfonate; nevertheless, similar performance was observed during the other periods when measurements were undertaken.

(3) The results deriving from LWD and DCP were in good agreement as both the test equipment indicated that the stabilized aggregates performed better than the untreated ones and that the mechanical response related to the investigated additive technologies gradually reduced over time.

(4) The test sections were built comprising aggregates that fulfilled the standard code requirements. Therefore, using the investigated nontraditional stabilizing agents can lead to even greater benefits for those "weak" aggregates that do not meet the requirements specified by the design manual.

As an input for future research efforts, some considerations can be made to indicate the directions to expand the investigation. Even if the test results of this study were positive, the outcomes could be generalized even more by employing other rock types. Moreover, mixing proportions containing different additive percentages as well as the exposure to different climates and temperatures could be investigated. Finally, compound modification of the polymer-based and lignin-based stabilizing agents could also be explored.

Data Availability

The data are available by contacting the corresponding author at diego.barbieri@ntnu.no.

Disclosure

The main results of this work were presented at "World Transport Convention 2021" (15–19 June 2021, Xi'an, China) with the title "Performance of road base layers stabilized with organosilane and lignosulfonate during a two-year time span."

Conflicts of Interest

The authors declare that there are no conflicts of interest regarding the publication of this paper.

Acknowledgments

References

[1] K. K. Dunham, "Coastal highway route E39 - extreme crossings," *Transportation Research Procedia*, vol. 14, pp. 494–498, 2016.

[2] NPRA, "The E39 coastal highway route," 2017, https://www.vegvesen.no/en/roads/Roads+and+bridges/Road+projects/e39coastalhighwayroute;jsessionid=99D143CB28F87A072777C744BBCA31E8?lang=nn.

[3] A. Gomes Correia, M. G. Winter, and A. J. Puppala, "A review of sustainable approaches in transport infrastructure geotechnics," *Transportation Geotechnics*, vol. 7, pp. 21–28, 2016.

[4] G. Petkovic, "Recycling in Norwegian conditions," in *Proceedings of the 5th International Conference Bear. Capacit. Roads Airfields, Tapir, Trondheim*, R. S. Nordal and G. Refsdal, Eds., , 2005.

[5] P. P. Riviera, R. Bellopede, P. Marini, and M. Bassani, "Performance-based re-use of tunnel muck as granular material for subgrade and sub-base formation in road construction," *Tunnelling and Underground Space Technology*, vol. 40, pp. 160–173, 2014.

[6] E. Hoxha, H. R. Vignisdottir, D. M. Barbieri et al., "Life cycle assessment of roads: exploring research trends and harmonization challenges," *The Science of the Total Environment*, vol. 759, p. 143506, 2021.

[7] D. M. Barbieri, B. Lou, F. Wang et al., "Assessment of carbon dioxide emissions during production, construction and use stages of asphalt pavements," *Transp. Res. Interdiscip. Perspect.*vol. 11, 2021.

[8] Teknologirådet, "Teknologirådet | norge 2030 arkiver," 2012, https://teknologiradet.no/category/norge-2030/.

[9] D. M. Barbieri, I. Hoff, and H. Mork, "Laboratory investigation on unbound materials used in a highway with premature damage," in *Proceedings of the 10th International Conference Bear. Capacit. Roads, Railw. Airfields*, Athens, Greece, June 2017.

[10] Npra, *Handbook N200 Vegbygging*, Vegdirektoratet, Oslo, Norway, 2018.

[11] Npra, *Handbook N200 Vegbygging*, Vegdirektoratet, Oslo, Norway, 2014.

[12] Cen, *I. S. O. 1097-2 Tests for Mechanical and Physical Properties of Aggregates. Part 2: Methods for the Determination of Resistance to Fragmentation*, Standard, Delhi, India, 2010.

[13] Cen, *I. S. O. 1097-1 Tests for Mechanical and Physical Properties of Aggregates. Part 1: Determination of the Resistance to Wear (Micro-deval)*, Standard, Delhi, India, 2011.

[14] S. Adomako, C. J. Engelsen, R. T. Thorstensen, and D. M. Barbieri, "Review of the relationship between aggregates geology and Los Angeles and micro-Deval tests," *Bulletin of Engineering Geology and the Environment*, 2021.

[15] D. M. Barbieri, I. Hoff, and M. B. E. Mørk, "Mechanical assessment of crushed rocks derived from tunnelling operations," in *Proceedings of the 5th GeoChina Internationl Conference 2018*, W.-C. Cheng, J. Yang, and J. Wang, Eds., pp. 225–241, Springer, HangZhou, China, July 2019.

[16] A. Behnood, "Soil and clay stabilization with calcium- and non-calcium-based additives: a state-of-the-art review of challenges, approaches and techniques," *Transportation Geotechnics*, vol. 17, pp. 14–32, 2018.

[17] Y. J. Jiang and L. F. Fan, "An investigation of mechanical behavior of cement-stabilized crushed rock material using different compaction methods," *Construction and Building Materials*, vol. 48, pp. 508–515, 2013.

[18] J. Myre, *The Use of Cold Bitumen Stabilized Base Course Mixes in Norway*, pp. 1–14, Vegdirektoratet, Oslo, Norway, 2014.

[19] NPRA, *Kalde Bitumen- Stabiliserte Bærelag*, Vegdirektoratet, Oslo, Norway, 2014.

[20] K. Siripun, P. Jitsangiam, and H. Nikraz, "Characterization analysis and design of hydrated cement treated crushed rock base as a road base material in Western Australia," *International Journal Pavement Reserach Technol.*vol. 10, pp. 39–47, 2010.

[21] Z. Liu, B. Lou, D. M. Barbieri, A. Sha, T. Ye, and Y. Li, "Effects of pre-curing treatment and chemical accelerators on Portland cement mortars at low temperature (5°C)," *Construction and Building Materials*, vol. 240, 2020.

[22] D. M. Barbieri, I. Hoff, and C.-H. Ho, "Crushed rocks stabilized with organosilane and lignosulfonate in pavement unbound layers: repeated load triaxial tests," *Frontiers of Structural and Civil Engineering*, 2021.

[23] D. M. Barbieri, I. Hoff, and M. B. E. Mørk, "Innovative stabilization techniques for weak crushed rocks used in road unbound layers: a laboratory investigation," *Transportation Geotechnics*, vol. 18, pp. 132–141, 2019.

[24] D. M. Barbieri, I. Hoff, and M. B. E. Mørk, "Organosilane and lignosulfonate as innovative stabilization techniques for crushed rocks used in road unbound layers," *Transp. Geotech.*vol. 22, 2020.

[25] D. P. Alazigha, B. Indraratna, J. S. Vinod, and A. Heitor, "Mechanisms of stabilization of expansive soil with lignosulfonate admixture," *Transportation Geotechnics*, vol. 14, pp. 81–92, 2018.

[26] Q. Chen, B. Indraratna, J. Carter, and C. Rujikiatkamjorn, "A theoretical and experimental study on the behaviour of lignosulfonate-treated sandy silt," *Computers and Geotechnics*, vol. 61, pp. 316–327, 2014.

[27] J. Daniels and M. S. Hourani, "Soil improvement with organosilane," *U.S.-China Work Government Improvement Technol.*, 2009.

[28] R. L. Santoni, J. S. Tingle, and S. L. Webster, "Stabilization of silty sand with nontraditional additives," *Transportation Research Record: Journal of the Transportation Research Board*, vol. 1787, no. 1, pp. 61–70, 2002.

[29] B. Ta'negonbadi and R. Noorzad, "Physical and geotechnical long-term properties of lignosulfonate-stabilized clay: an experimental investigation," *Transp. Geotech.*vol. 17, pp. 41–50, 2018.

[30] O. O. Ugwu, J. B. Arop, C. U. Nwoji, and N. N. Osadebe, "Nanotechnology as a preventive engineering solution to highway infrastructure failures," *Journal of Construction Engineering and Management*, vol. 139, no. 8, pp. 987–993, 2013.

[31] T. Zhang, G. Cai, and S. Liu, "Application of lignin-stabilized silty soil in highway subgrade: a macroscale laboratory study," *Journal of Materials in Civil Engineering*, vol. 30, 2018.

[32] D. M. Barbieri, M. Tangerås, E. Kassa, I. Hoff, Z. Liu, and F. Wang, "Railway ballast stabilising agents: comparison of mechanical properties," *Construction and Building Materials*, vol. 252, 2020.

[33] ASTM International, *Standard Test Method for Measuring Deflections Using a Portable Impulse Plate Load Test Device*, ASTM International, West Conshohocken, PA, USA, 2015.

[34] ASTM International, *Standard Test Method for Use of the Dynamic Cone Penetrometer in Shallow Pavement Applications*, ASTM International, West Conshohocken, PA, USA, 2018.

[35] T. Grenne, G. Grammeltvedt, and F. M. Vokes, "Ophiolites type sulphide deposits in the western Trondheim district, central Norwegian caledonides," in *Proceedings of the International Ophiolite Symposium*, pp. 727–743, Geological Survey Department, Nicosia, Cyprus, 1980.

[36] G. Petkovic, C. J. Engelsen, A.-O. Håøya, and G. Breedveld, "Environmental impact from the use of recycled materials in road construction: method for decision-making in Norway," *Resources, Conservation and Recycling*, vol. 42, no. 3, pp. 249–264, 2004.

[37] CEN, *ISO 14688-1 Geotechnical Investigation and Testing. Identification and Classification of Soil*, International Organization for Standardization (ISO), Geneva, Switzerland, 2018.

[38] CEN, *ISO 13286-4 Test Methods for Laboratory Reference Density and Water Content - Vibrating Hammer*, International Organization for Standardization (ISO), Geneva, Switzerland, 2003.

[39] J. S. Tingle, J. K. Newman, S. L. Larson, C. A. Weiss, and J. F. Rushing, "Stabilization mechanisms of nontraditional additives," *Transportation Research Record: Journal of the Transportation Research Board*, vol. 1989-2, no. 1, pp. 59–67, 2007.

[40] B. K. Kunz, E. E. Little, and V. L. Barandino, "Aquatic toxicity of chemical road dust suppressants to freshwater organisms," *Archives of Environmental Contamination and Toxicology*, vol. 2, 2021.

[41] DD CEN/TS, *Characterization of Waste. Leaching Behaviour Tests. Up-Flow Percolation Test*, under specified conditions, 2006.

[42] D. Jones, "Guidelines for the selection, specification, and application of chemical dust control and stabilization treatments on unpaved roads," 2017, https://escholarship.org/uc/item/0347c9zj.

[43] A. A. Fungaroli and S. R. Prager, "Evaluation of some acrylic polymers as soil stabilizers," *Product R&D*, vol. 8, no. 4, pp. 450–453, 1969.

[44] Y. Ohama, "Polymer-based admixtures," *Cement and Concrete Composites*, vol. 20, no. 2-3, pp. 189–212, 1998.

[45] E. H. Tan, E. M. M. Zahran, and S. J. Tan, "A review of chemical stabilisation in road construction," *IOP Conference Series: Materials Science and Engineering*, vol. 943, 2020.

[46] D. Jones and R. Surdahl, "New procedure for selecting chemical treatments for unpaved roads," *Transportation Research Record: Journal of the Transportation Research Board*, vol. 2433, no. 1, pp. 87–99, 2014.

[47] M. C. Roco, "Broader societal issues of nanotechnology," *Journal of Nanoparticle Research*, vol. 5, no. 3/4, pp. 181–189, 2003.

[48] K. Sobolev, "Modern developments related to nanotechnology and nanoengineering of concrete," *Frontiers of Structural and Civil Engineering*, vol. 10, no. 2, pp. 131–141, 2016.

[49] K. Sobolev and S. P. Shah, *Nanotechnology in Construction Proc. NICOM5*, K. Sobolev and S. P. Shah, Eds., p. 509, Springer, NEW York, NY, USA, 2015.

[50] S. R. Wasserman, Y. T. Tao, and G. M. Whitesides, "Structure and reactivity of alkylsiloxane monolayers formed by reaction of alkyltrichlorosilanes on silicon substrates," *Langmuir*, vol. 5, no. 4, pp. 1074–1087, 1989.

[51] H. K. Kim, J. P. Lee, C. R. Park, H. T. Kwak, and M. M. Sung, "Thermal decomposition of alkylsiloxane self-assembled monolayers in air," *The Journal of Physical Chemistry B*, vol. 107, no. 18, pp. 4348–4351, 2003.

[52] T. Zhang, Y. L. Yang, and S. Y. Liu, "Application of biomass by-product lignin stabilized soils as sustainable geomaterials: a review," *The Science of the Total Environment*, vol. 728, Article ID 138830, 2020.

[53] G. Dondi, C. Sangiorgi, and C. Lantieri, "Applying geostatistics to continuous compaction control of construction and demolition materials for road embankments," *Journal of Geotechnical and Geoenvironmental Engineering*, vol. 140, no. 3, Article ID 06013005, 2014.

[54] C. Sangiorgi, C. Lantieri, and G. Dondi, "Construction and demolition waste recycling: an application for road construction," *International Journal of Pavement Engineering*, vol. 16, no. 6, pp. 530–537, 2015.

[55] HMP-LFG, *The Light Drop Weight Tester*, Magdeburg prufgeratebau GmbH, Magdeburg, Germany, 2018, https://www.hmp-online.com/en/.

[56] HMP-LFG, *HMP-LFG4 Instruction Manual*, Magdeburg prufgeratebau GmbH, Magdeburg, Germany, 2017.

[57] H. Chennarapu, T. K. Garala, R. Chennareddy, U. Balunaini, and G. Venkata Narasimha Reddy, "Compaction quality control of earth fills using dynamic cone penetrometer," *Journal of Construction Engineering and Management*, vol. 144, no. 9, Article ID 04018086, 2018.

[58] J. Boussinesq, *Application des potentiels a l'etude de l'equilibre et du mouvement des Solids Elastiques*, Gauthier-Villars, Paris, France, 1885.

[59] P. Vennapusa and D. White, "Comparison of light weight deflectometer measurements for pavement foundation materials," *Geotechnical Testing Journal*, vol. 32, 2009.

[60] P. Fleming, M. Frost, and J. Lambert, "Review of lightweight deflectometer for routine in situ assessment of pavement material stiffness," *Transport Research Record Journal Transport Research Board.*, pp. 80–87, 2004.

[61] M. A. Mooney and P. K. Miller, "Analysis of lightweight deflectometer test based on in situ stress and strain response," *Journal of Geotechnical and Geoenvironmental Engineering*, vol. 135, no. 2, pp. 199–208, 2009.

[62] D. H. Chen, D. Lin, P. Liau, and J. Bilyeu, "A correlation between dynamic cone penetrometer values and pavement layer moduli," *Geotechnical Testing Journal*, vol. 28, 2005.

[63] J. Chen, M. Hossain, and T. M. Latorella, "Use of falling weight deflectometer and dynamic cone penetrometer in pavement evaluation," *Transportation Research Record: Journal of the Transportation Research Board*, vol. 1655, no. 1, pp. 145–151, 1999.

[64] J. Siekmeier, D. Young, and D. Beberg, "Comparison of the dynamic cone penetrometer with other tests during subgrade and granular base characterization in Minnesota," in *Nondestruct. Test. Pavements Backcalc. Modul. 3rd Vol*, S. D. Tayabji and E. O. Lukanen, Eds., American Society for Testing Materials, West Conshohocken, PA, USA, 2000.

[65] Norwegian Meteorological Institute, "eKlima," 2020, http://sharki.oslo.dnmi.no/portal/page?_pageid73,=39035,73_39049&_dad=portal&_schema=PORTAL.

[66] US National Weather Service, "Precipitation measurements," 2020, https://www.weather.gov/abrfc/map.

[67] CEN, "ISO 11272 Soil quality - determination of dry bulk density," 2017, https://www.iso.org/standard/68255.html.

[68] A. S. Norsk rikskringkasting, "Varmerekord i Sør-Norge i mai," 2018, https://www.nrk.no/hordaland/varmerekord-i-sor-norge-i-mai-1.14054641.